

Microstructure, ferroelectric and dielectric proprieties of $\text{Bi}_4\text{Ti}_3\text{O}_{12}$ materials prepared by two methods

Min Shi¹ · Yafeng Shi¹ · Ruzhong Zuo¹ · Yudong Xu¹ · Xudong Peng¹ · Di Li¹ · Liexiang Xie¹

Received: 8 September 2015 / Accepted: 29 November 2015 / Published online: 11 December 2015
© Springer Science+Business Media New York 2015

Abstract $\text{Bi}_4\text{Ti}_3\text{O}_{12}$ (BTO) materials were prepared by the sol–gel method via the acetic acid method (AAM) or the ethylene glycol method (EGM). BTO powders prepared by EGM are composed of the main phase without purity phases when annealed at 650 °C. BTO powders prepared by AAM are composed of the main phase without secondary phases when annealed at 625 °C. BTO ceramics prepared by AAM have denser microstructure and greater grain size than those prepared by EGM. BTO ceramics prepared by two methods exhibit well typical P–E loops for ferroelectrics. The remnant polarization of BTO ceramics prepared by AAM is greater than those prepared by EGM. And the coercive field and dielectric loss of BTO ceramics prepared by AAM are smaller than those prepared by EGM. BTO ceramics prepared by AAM have better ferroelectric and dielectric properties than those prepared by EGM.

1 Introduction

Lead-based ferroelectric materials, such as $\text{Pb}(\text{Zr}, \text{Ti})\text{O}_3$, have been widely used as actuator, sensor, and transducer due to their excellent ferroelectric and piezoelectric properties [1, 2]. However, it is generally accepted that lead is hazardous to environments and human health [3–7]. Therefore, it is urgent to develop lead-free ferroelectric materials with good dielectric and ferroelectric properties [8–12]. The main lead-free materials are BiFeO_3 [13, 14], BaTiO_3 [15–18], (K, Na) NbO_3 [19, 20] and $\text{Bi}_4\text{Ti}_3\text{O}_{12}$

[21–24] based materials. BiFeO_3 based materials have high Curie temperature and high Neel temperature. However, high electric leakage in bulk BiFeO_3 based materials was observed due to the existence of multivalent Fe ions and oxygen vacancies [15]. BaTiO_3 based materials have low Curie temperature (120 °C) and modest piezoelectric properties which are greatly inferior to PZT [25–27]. And dielectric properties of them undergo tremendous changes around Curie temperature [28]. $\text{K}_x\text{Na}_{1-x}\text{NbO}_3$ (KNN) based materials have high Curie temperature and good ferroelectric and piezoelectric properties. The main disadvantage of KNN based materials is low value of d_{33} . And another disadvantage is difficulty in maintaining stoichiometry due to high volatilization of Na and K, which lead to the formation of impurity phases [29]. $\text{Bi}_4\text{Ti}_3\text{O}_{12}$ based materials is one of the most promising ferroelectric materials for their high dielectric constant, low sintering temperature, significant ferroelectric properties and high piezoelectric properties [30–32]. Peng [33] and Chen [34] prepared $\text{Bi}_4\text{Ti}_{2.9}\text{W}_{0.05}\text{Nb}_{0.05}\text{O}_{12}$ ceramics by the solid-state reaction method. Bokolia et al. [35] also prepared $\text{Bi}_{4-x}\text{Er}_x\text{Ti}_3\text{O}_{12}$ ($x = 0.0, 0.05, 0.1, 0.2$ and 0.3) ceramics by the conventional solid-state reaction method. Up to date, $\text{Bi}_4\text{Ti}_3\text{O}_{12}$ ferroelectric materials were mainly prepared by the solid-state reaction method. The conventional solid-state reaction method has some disadvantages, such as higher sintering temperature, longer sintering time, larger grain size [36–38]. However, the sol–gel method has several advantages such as the precise control of chemical composition, better homogeneity, low processing temperature, low cost, very fine particle sizes. [37–39]. Very few literatures have reported on the synthesis of $\text{Bi}_4\text{Ti}_3\text{O}_{12}$ materials via the sol–gel method. Furthermore, the researches about the influence of different solvents on the ferroelectric properties of $\text{Bi}_4\text{Ti}_3\text{O}_{12}$ materials are lacking. In

✉ Min Shi
mrshimin@hotmail.com

¹ School of Materials Science and Engineering, Hefei University of Technology, Hefei, Anhui, China

this study, $\text{Bi}_4\text{Ti}_3\text{O}_{12}$ materials were prepared by the sol-gel method via two methods (EGM and AAM). Impact of different solvents on the phase constitution, microstructures, ferroelectric and dielectric properties of $\text{Bi}_4\text{Ti}_3\text{O}_{12}$ materials systematically was investigated.

2 Experiment details

$\text{Bi}_4\text{Ti}_3\text{O}_{12}$ (BTO) materials were prepared by sol-gel method using analytical reagent (AR) grade chemicals (purity >99 %). The mole ratio of Bi^{3+} and Ti^{4+} is 4.4:3. 10 mol% excess Bi is required to compensate for volatile of Bi during annealing progress. Two methods to prepare BTO materials were adopted via different solvents.

For the first method, the appropriate portions of Bismuth nitrate pentahydrate ($\text{Bi}(\text{NO}_3)_3 \cdot 5\text{H}_2\text{O}$), was dissolved in acetic acid, stirred at 60 °C for 30 min. Tetrabutyl titanate ($(\text{C}_4\text{H}_9\text{O})_4$) was dissolved in ethylene glycol methyl ether. Acetic acid was added to prevent the formation of precipitation. Two solutions were mixed and stirred at 45 °C for 6 h to obtain a stable precursor sol of BTO. This method was named the acetic acid method (AAM) according to the solvent, acetic acid.

For the second method, the appropriate portions of $\text{Bi}(\text{NO}_3)_3 \cdot 5\text{H}_2\text{O}$ was dissolved in ethylene glycol, stirred at 60 °C for 30 min. Tetrabutyl titanate ($\text{Ti}(\text{C}_4\text{H}_9\text{O})_4$) was dissolved in ethylene glycol methyl ether. Acetic acid was added to prevent the formation of precipitation. Two solutions were mixed and stirred at 45 °C for 6 h to obtain another stable precursor sol of BTO. This method was named the ethylene glycol method (EGM).

The precursor sols of BTO prepared by above two methods were annealed at different temperatures to investigate the impact of annealing temperatures on phase constitutions of BTO powders. Two precursor sols of BTO prepared by the two methods were dried at 120 °C for 48 h and ground to obtain two kinds of powders. The powders were annealed at 650 °C to obtain pure two kinds of BTO powders. The polyvinyl alcohol (the mass fraction is 3 %) was then added to obtain two kinds of mixtures. Then the two mixtures were ground evenly and compressed into two kinds of flakes with thickness 1 mm and diameter 10 mm. Lastly, the flakes were caked at 900 °C to obtain two kinds of ceramic samples.

The thermal behavior of powders was explored by differential scanning calorimetry and thermal gravimetric analyzer (STA449F3, Netzsch, Germany). Phase constitutions of the powders were characterized by X-ray diffractometer (XRD, D/MAX2500 V, Rigaku, Japan) with $\text{CuK}\alpha$ radiation. The microstructures of BTO powders were determined by transmission electron microscope (TEM, H800, Hitachi, Japan). The size distributions of particles

were surveyed by laser particle size analyzer (MS-2000, Malvern, United Kingdom). The Raman spectrum of the powders was characterized by microscopic confocal laser Raman spectrometer (HR Evolution, Horiba Jobin-Yvon, France). The surface morphologies of BTO ceramics were assessed by field emission scanning electron microscopy (FE-SEM, SU8020, Hitachi, Japan). In order to measure electric properties, BTO ceramic samples were polished and painted with silver pastes on the two sides and then fired at 600 °C for 10 min. BTO ceramic samples were poled at a dc field of 40 kV/cm for 30 min. The ferroelectric hysteresis loops of the samples were measured at room temperature using a multiferroic tester system (MultiFerroic100 V, Radiant Technology, USA). The dielectric loss of BTO ceramic samples were characterized by the capacitance resistance meter (4980A, Agilent, USA).

3 Results and discussion

The curves of differential scanning calorimetry (DSC) and thermal gravimetric (TG) analyzer of BTO powders prepared by two methods were shown in Fig. 1. From Fig. 1a, it can be seen that there exists the exothermic peak at about 210 °C in BTO powders prepared by EGM, indicating the volatilization of ethylene glycol. And there is a small weight loss (−8.36 %) ranging from room temperature to 210 °C. The sharp exothermic peaks at 238 and 271 °C are attributed to the thermal decomposition of nitrate and organic combustion, along with a sharp weight loss (−15.68 %). The exothermic peak at 397 °C, with a small weight loss (−4.95 %), indicates the decomposition of the remaining nitrate. And there is no significant weight loss above 505 °C, which implies that there is no significant phase transformation above 505 °C. From the Fig. 1b, it is clear that there exist peaks at 85 and 200 °C in BTO powders prepared by EGM which are due to the loss of water in $\text{Bi}(\text{NO}_3)_3 \cdot 5\text{H}_2\text{O}$ and the volatilization of the organic solvents (acetic acid and ethylene glycol methyl ether), respectively, along with a 5.99 % weight loss from room temperature to 200 °C. There are two sharp exothermic peaks near 298 and 320 °C corresponding to the thermal decomposition of nitrate and organic combustion, with a significant weight loss (21.39 %). The peak at 505 °C may be attributed to the crystallization of precursor.

The X-ray diffractions (XRD) of BTO powders prepared by two methods were shown in the Fig. 2. Figure 2a illustrates that BTO powders (prepared by EGM) when annealed at 550 °C contain more amount of impurity phase (TiO_2) besides the main phase ($\text{Bi}_4\text{Ti}_3\text{O}_{12}$) with perovskite structure. With the increase of annealing temperatures, the relative amounts of impurity phase decreases remarkably.

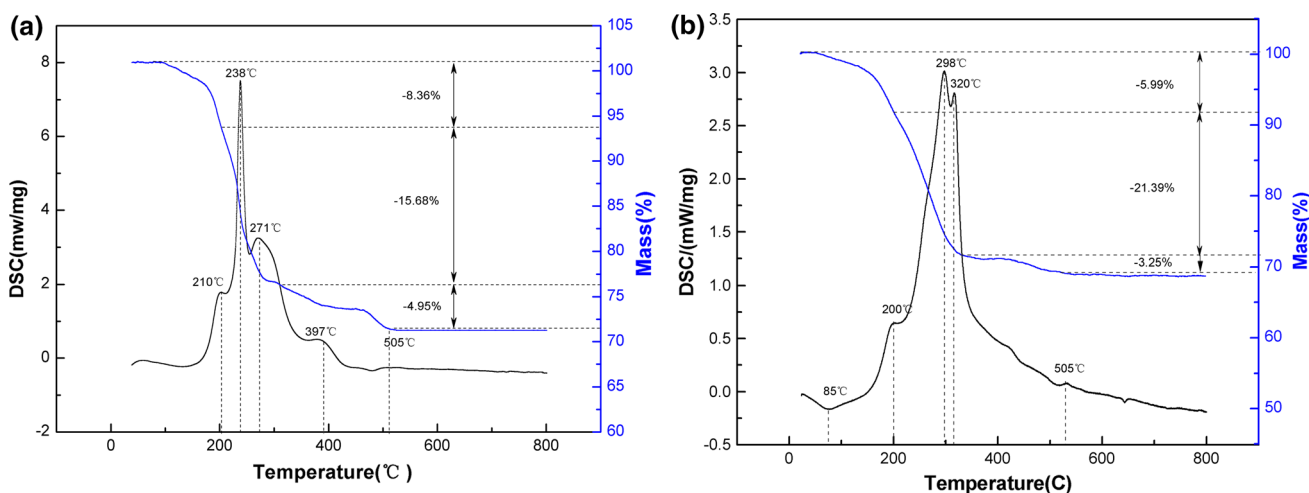


Fig. 1 DSC and TG curves of BTO powders prepared by **a** EGM; **b** AAM

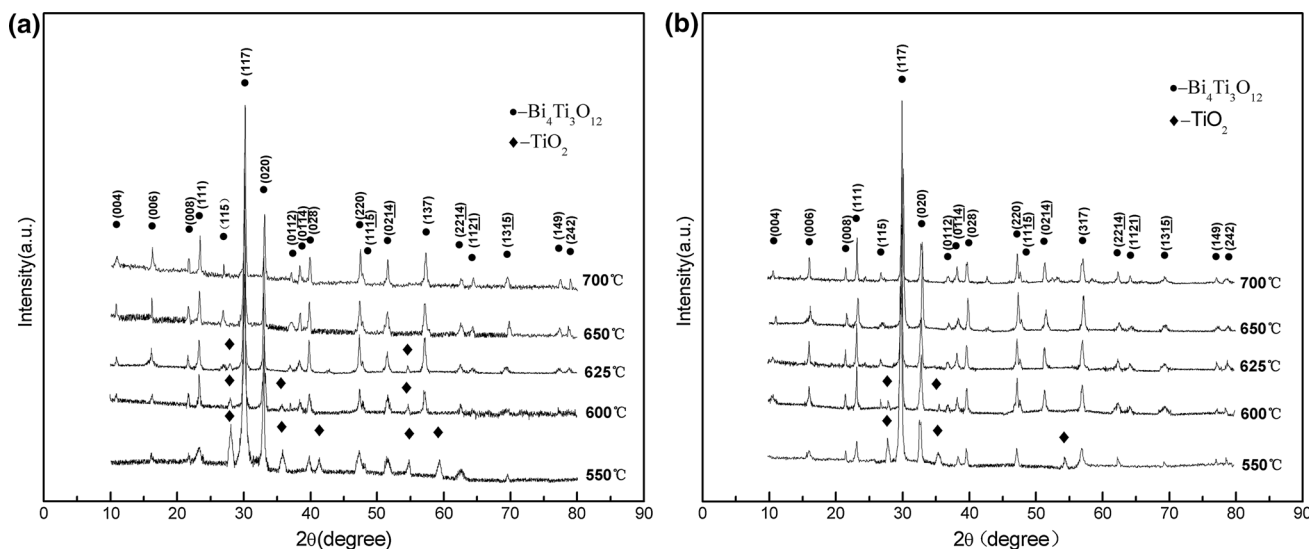


Fig. 2 XRD patterns of BTO powders, annealed at different temperatures, prepared by **a** EGM; **b** AAM

And there is still a small amount of impurity phase when annealed at 625 °C. And no impurity phases can be detected within the sensitivity of XRD when the annealing temperature reaches 650 °C. Figure 2b shows that there is much more amount of impurity phase (TiO₂) besides the main phase (Bi₄Ti₃O₁₂) with perovskite structure in BTO powders (prepared by AAM) annealed at 550 °C. With the increase of annealing temperatures, the relative amounts of impurity phase decreases gradually. And no impurity phase can be found when annealing temperature reaches 625 °C. Therefore, BTO powders with pure BTO can be obtained at the lower annealing temperature by AAM not EGM.

Figure 3 illustrated the TEM micrographs of BTO powders prepared by EGM. The powders with fine particle sizes can be seen. With the increase of annealing temperatures, the particle grain sizes increase. The average particle size of BTO

powders prepared by EGM, which are annealed at 650 °C, is about 30 nm. Figure 4 illustrates the TEM micrographs of BTO powders prepared by AAM. It is indicated that coarse size particles and agglomeration exist in BTO powders prepared by AAM. And average particle size of BTO powders prepared by AAM, which are annealed at 650 °C, is about 1.2 μm. It is clear that the particle sizes of BTO powders prepared by EGM are smaller than those of BTO powders prepared by AAM at the same annealing temperature.

The size distributions of particles of two kinds of powders, annealed at 650 °C, were showed in Fig. 5. Particle sizes of powders prepared by the two methods were listed in Table 1. It can be seen that the powder prepared by AAM have larger particle size than that prepared by EGM, which is consistent with above-mentioned TEM results.

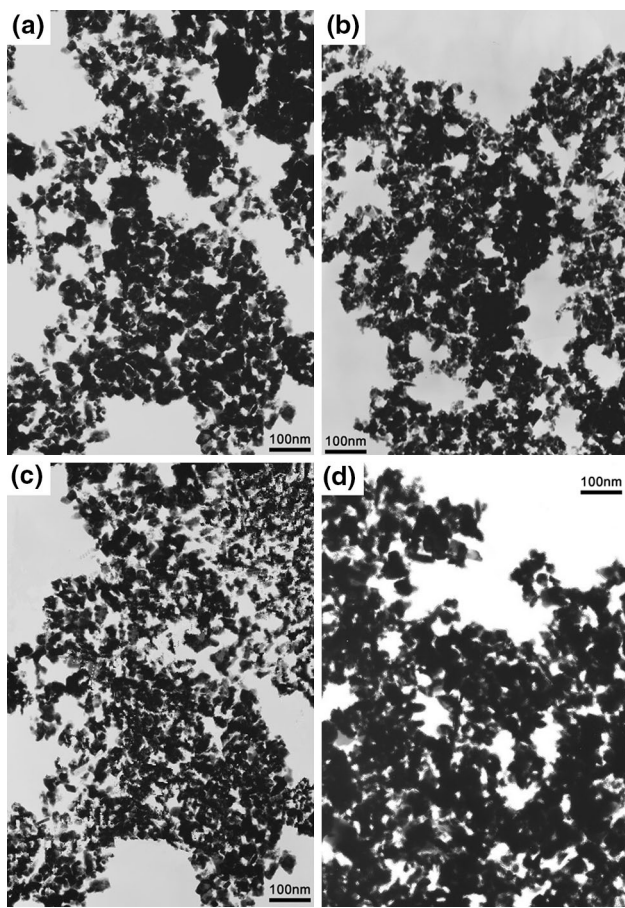


Fig. 3 TEM micrographs of BTO powders, prepared by EGM, annealed at different temperatures **a** 550 °C; **b** 600 °C; **c** 650 °C; **d** 700 °C

The Raman spectra of BTO powders prepared by two methods were exhibited in the Fig. 6. It is clear that the two powders have similar peaks. Strong interactions between atoms, which mainly arise from the stretching and bending of the shorter metal–oxygen bonds within the anionic groups, will form stronger Raman peaks [40]. According to data of $\text{Bi}_4\text{Ti}_3\text{O}_{12}$ [41], the Raman phonon peak observed at 849 cm^{-1} is ascribed to the symmetric Ti–O stretching in TiO_6 octahedra, which originates mainly from the vibrations of atoms inside the TiO_6 octahedra. The peaks at 537 cm^{-1} (TO) and 618 cm^{-1} (LO) are ascribed to O–Ti–O stretching vibrations. They split into a longitudinal (LO) and transverse (TO) components due to the long-range electrostatic forces that might be associated with lattice ionicity [42]. The 267 and 231 cm^{-1} peaks are ascribed to the O–Ti–O bending vibrations. The peak at 310 cm^{-1} is attributed to a combination of stretching and bending vibrations. The peak at 194 cm^{-1} is observed due to the distortion of TiO_6 octahedra. The distortion may result from the strain or oxygen vacancies, which are commonly

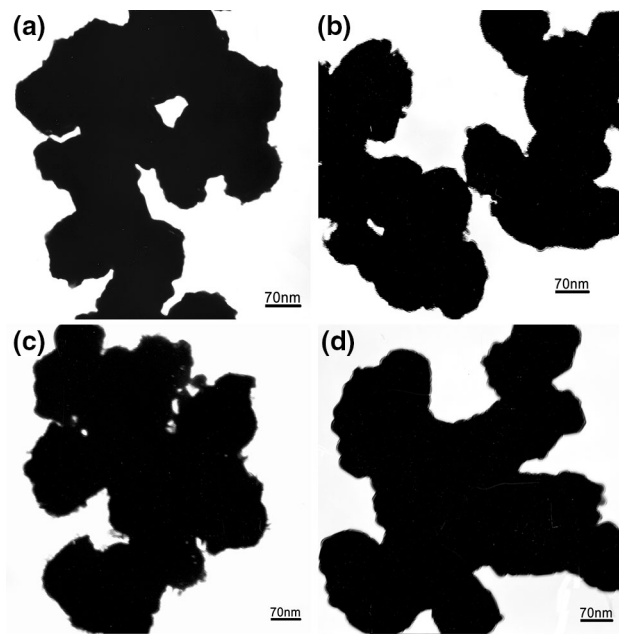


Fig. 4 TEM micrographs of BTO powders, prepared by AAM, annealed at different temperatures **a** 550 °C; **b** 600 °C; **c** 650 °C; **d** 700 °C

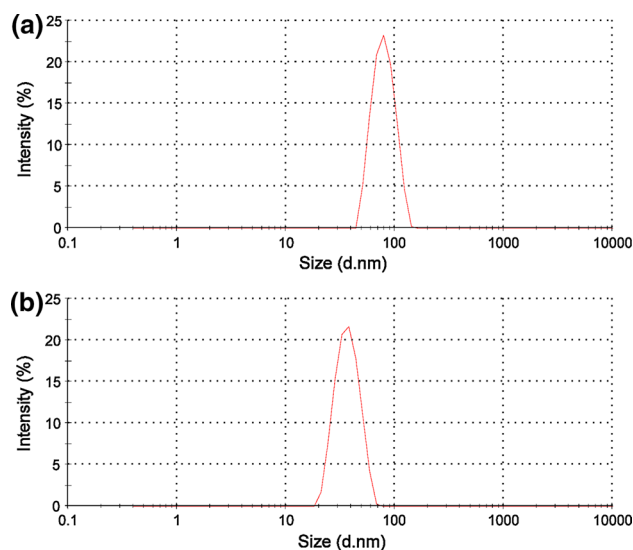


Fig. 5 Size distribution of BTO powders, annealed at 650 °C, prepared by **a** EGM; **b** AAM

accepted as the cause of fatigue behaviour in Bi layered perovskite. The peak at 116 cm^{-1} is attributed to the vibrations between Bi and O atoms. The existence of the peaks at 267, 537, and 849 cm^{-1} confirms the presence of perovskite structure. This is consistent with XRD results of BTO powders.

Figure 7 shows the FESEM images of the surfaces of BTO ceramics prepared by two methods. It is seen from

Table 1 Particle size of powders prepared by the two methods

Powders prepared by	Average size (nm)	Peak width (nm)	Main peak (nm)
EGM	37.44	9.153	37.44
AAM	76.23	18.36	80.35

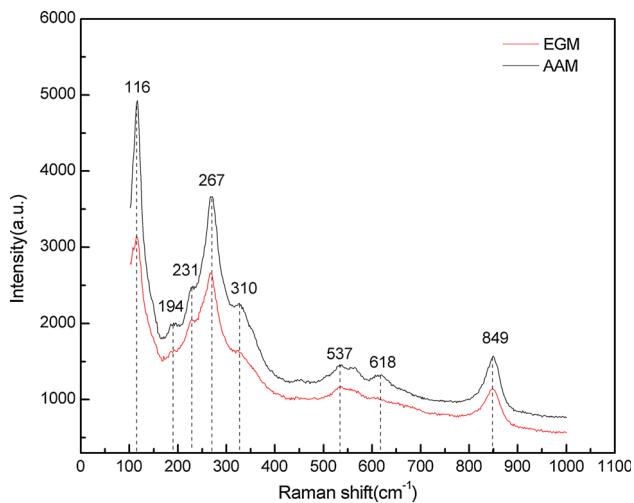
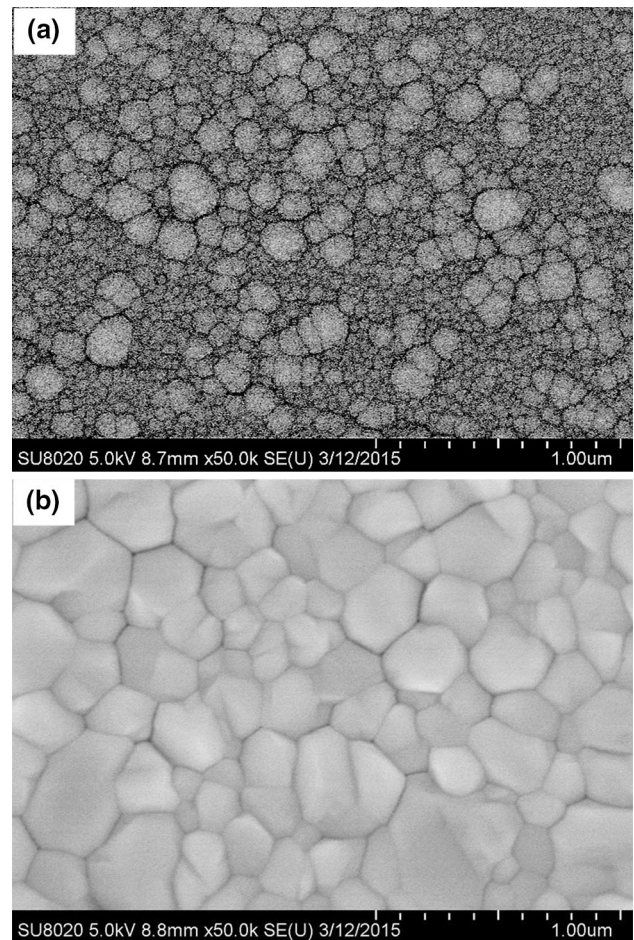
**Fig. 6** Raman spectrum of BTO powders prepared by EGM or AAM, annealed at 650 °C

Fig. 7a that BTO ceramics prepared by EGM have pores and microcracks without obvious grain boundaries. However from Fig. 7b, it is clear that BTO ceramics prepared by AAM have hexagonal grains and obvious grain boundaries, which indicating relative complete crystallization. It can also be seen that they also possess more compact microstructure without obvious pores and microcracks. The average grain size is about 1.3 μm . By comparing Fig. 7b with Fig. 7a, it is clear that BTO ceramics prepared by AAM has denser microstructure and greater grain size than those prepared by EGM.

The P–E loops of two kinds of BTO ceramics prepared by two methods were shown in Fig. 8. It is clear that two ceramics exhibit well typical P–E loops for ferroelectrics. The values of remnant polarizations (P_r), saturation polarizations (P_s) and coercive fields (E_c) drawn from Fig. 8 were listed in Table 2. It is found that values of P_r and P_s of BTO ceramics prepared by AAM are greater than those of BTO ceramics prepared by EGM. And the value of E_c of BTO ceramics prepared by AAM is smaller than that prepared by EGM. This means that BTO ceramics prepared by AAM have better ferroelectric properties. The enhancement of ferroelectricity could be attributed to the following reasons. On one hand, the polarization reversal process of ferroelectric domain in larger grains is much easier than that in small grains [43–48]. Therefore, BTO ceramics prepared by AAM with larger grains will possess better ferroelectricity. On the other hand,

**Fig. 7** FESEM micrographs of the surfaces of BTO ceramics, annealed at 650 °C, prepared by **a** EGM; **b** AAM

better crystallization, more compact microstructure and fewer defects will also help to improve the ferroelectricity of BTO ceramics prepared by AAM. The value of P_r of BTO ceramics prepared by AAM is much greater than that of BTO ceramics prepared by other researchers ($P_r = 13.0 \mu\text{C}/\text{cm}^2$ [31] and $P_r = 13.4 \mu\text{C}/\text{cm}^2$ [33]).

Figure 9 presents the dielectric loss ($\text{Tan}\delta$) of BTO ceramics prepared by two methods under different frequencies. It is seen that, with the increase of frequency, the values of $\text{Tan}\delta$ decrease sharply firstly, then decrease gradually and remain almost unchanged. At the same frequency, BTO ceramics prepared by AAM have lower values of $\text{Tan}\delta$, which may be due to greater grain size. This implies that BTO ceramics prepared by AAM have better dielectric properties.

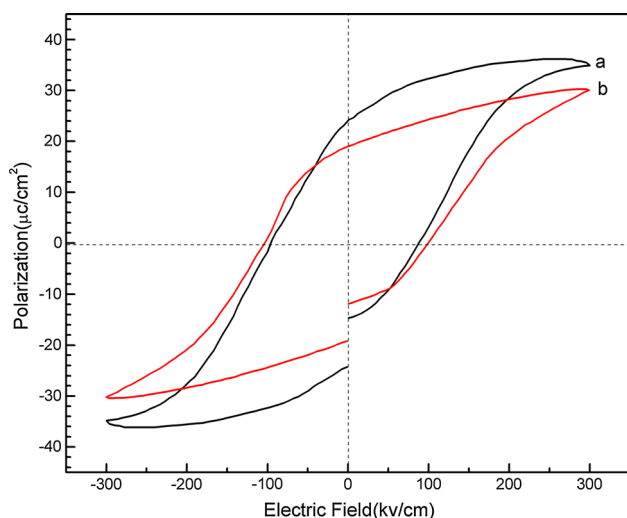


Fig. 8 P-E curves of BTO ceramics, annealed at 650 °C, prepared by **a** AAM; **b** EGM

Table 2 The ferroelectric parameters of two powders

Prepared by	Pr ($\mu\text{C}/\text{cm}^2$)	Ps ($\mu\text{C}/\text{cm}^2$)	Ec (kV/cm)
EGM	18.89	8.0	100.12
AAM	24.15	12.2	88.23

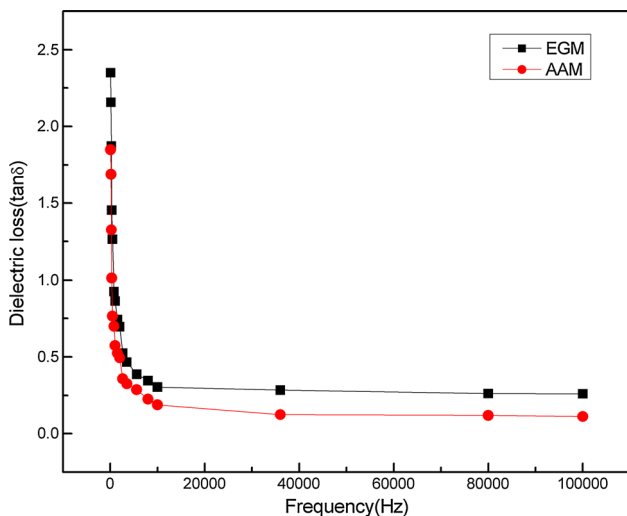


Fig. 9 Dielectric loss of BTO ceramics, annealed at 650 °C, prepared by **a** AAM; **b** EGM

4 Conclusions

BTO materials were prepared by the sol-gel method via two methods (EGM and AAM). With the increase of annealing temperatures, the relative amounts of impurity

phase decreases remarkably. BTO powders prepared by EGM are composed of the main phase without secondary phases when annealed at 650 °C. BTO powders prepared by AAM are composed of the main phase without secondary phase when annealed at 625 °C. BTO ceramics prepared by AAM have denser microstructure and greater grain size than those prepared by EGM. BTO ceramics prepared by two methods exhibit well typical P-E loops for ferroelectrics. The value of Pr of BTO ceramics prepared by AAM is greater than that of BTO ceramics prepared by EGM. And values of Ec and Tan δ of BTO ceramics prepared by AAM are smaller than those of BTO ceramics prepared by EGM. BTO ceramics prepared by AAM have better ferroelectric and dielectric properties.

Acknowledgments This work was supported by Anhui Provincial Natural Science Foundation (1308085ME59), Nippon Sheet Glass Foundation for Materials Science and Engineering of Japan (2012QTXM0079), the National Natural Science Foundation of China (51272060, 51472069).

References

- M.Y. Deng, X.L. Li, Z.H. Zhao, T. Li, Y.J. Dai, H.M. Ji, *J. Mater. Sci. Mater. El.* **25**, 1873–1879 (2014)
- J.Y. Chen, Y. Qi, W. Gao, Y.L. Bai, C.H. Nie, S.F. Zhao, *Mater. Lett.* **136**, 11–14 (2014)
- X.S. Lv, C.P. Cheng, Y.G. Xiao, M.H. Tang, Z.H. Tang, H.Q. Cai, Y.C. Zhou, R.W. Li, *Mater. Lett.* **100**, 7–10 (2013)
- K. Drogowska, S. Flege, D. Rogalla, H.W. Becker, E. Lonescu, N.T.H. Kim-Ngan, A.G. Balogh, *Solid State Ion.* **235**, 32–35 (2013)
- P.E. Janolin, *J. Mater. Sci.* **44**, 5025–5048 (2009)
- Q.H. Deng, Y.C. Fan, L.J. Wang, Z. Xiong, H.Z. Wang, Y.G. Li, Q.H. Zhang, A. Kawasaki, W. Jiang, *Jpn. J. Appl. Phys.* **51**(1R), 011501 (2012)
- K.P. Chen, F.L. Zhang, J.Q. Zhou, X.W. Zhang, C.W. Li, L.A. An, *Ceram. Int.* **41**, 10232–10236 (2015)
- P.K. Panda, Review: environmental friendly lead-free piezoelectric materials. *J. Mater. Sci.* **44**, 5049–5062 (2009)
- J. Rodel, W. Jo, K.T.P. Seifert, E.M. Anton, T. Granzow, D. Damjanovic, *J. Am. Ceram. Soc.* **92**, 1153–1177 (2009)
- J. Roedel, K.G. Webber, R. Dittmer, W. Jo, M. Kimura, D. Damjanovic, *J. Eur. Ceram. Soc.* **35**, 1659–1681 (2015)
- K. Kumar, N. Sinha, S. Bhandari, B. Kumar, *Ceram. Int.* **41**, 10237–10242 (2015)
- T. Takenaka, H. Nagata, *J. Eur. Ceram. Soc.* **25**, 2693–2700 (2005)
- T.P. Gujar, V.R. Shinde, S.S. Kulkarni, H.M. Pathan, C.D. Lokhande, *Appl. Surf. Sci.* **252**, 3585–3590 (2006)
- S.H. Jo, S.G. Lee, S.H. Lee, *Mater. Res. Bull.* **47**, 409–412 (2012)
- S.C. Yang, A. Kumar, V. Petkov, S. Priya, *J. Appl. Phys.* **113**, 144101 (2013)
- R.F. Zhang, C.Y. Deng, L. Ren, Z. Li, J.P. Zhou, *J. Electron. Mater.* **43**, 1043–1047 (2014)
- A.I. Ali, K. Park, A. Ullah, R. Huh, Y.S. Kim, *Thin Solid Films* **551**, 127–130 (2014)
- V.S. Puli, D.K. Pradhan, D.B. Chrisey, M. Tomozawa, G.L. Sharma, J.F. Scott, R.S. Katiyar, *J. Mater. Sci.* **48**, 2151–2157 (2013)
- R.A. Bucur, I. Badea, A.I. Bucur, S. Novaconi, *J. Alloy. Compd.* **630**, 43–47 (2015)

20. J. Schiemer, R.L. Withers, Y. Liu, Z.G. Yi, J. Solid State Chem. **195**, 55–62 (2012)
21. B.C. Sun, H. Wang, J.W. Xu, L. Yang, S.J. Zhou, Y.P. Zhang, Z.D. Li, Microelectron. Eng. **113**, 1–4 (2014)
22. D. Thomazini, M.V. Gelfuso, J.A. Eiras, Powder Technol. **222**, 139–142 (2012)
23. M. Roy, I. Bala, S.K. Barbar, S. Jangid, P. Dave, J. Phys. Chem. Solids **72**, 1347–1353 (2011)
24. V.B.D. Santos, J.C.M. Peko, V.R. Mastelaro, J. Alloy. Compd. **510**, 60–65 (2012)
25. M. Aghayan, A.K. Zak, M. Behdani, A.M. Hashim, Ceram. Int. **40**, 16141–16146 (2014)
26. S. Sharma, K. Shamim, A. Ranjan, R. Rai, P. Kumari, S. Sinha, Ceram. Int. **41**, 7713–7722 (2015)
27. P. Zheng, J. Zhang, Y. Tan, C. Wang, Acta Mater. **60**, 5022–5030 (2012)
28. C. Chen, H.R. Zhuang, X.N. Zhu, K.C. Zhou, D. Zhang, Ceram. Int. **41**, 9893–9898 (2015)
29. M. Chandraiah, P.K. Panda, Ceram. Int. **41**, 8040–8045 (2015)
30. Y. Zhang, L.Q. Wang, D.F. Xue, Powder Technol. **217**, 629–633 (2012)
31. T. Wei, C.Z. Zhao, C.P. Li, Y.B. Lin, X. Yang, H.G. Tan, J. Alloy. Compd. **577**, 728–733 (2013)
32. C.S. Chou, R.Y. Yang, J.H. Chen, S.W. Chou, Powder Technol. **199**, 264–271 (2010)
33. Z.H. Peng, Q. Chen, Y. Chen, D.Q. Xiao, J.G. Zhu, Mater. Res. Bull. **59**, 125–130 (2014)
34. Z.H. Chen, J.F. Qiu, C. Liu, J.N. Ding, Y.Y. Zhu, Ceram. Int. **36**, 241–244 (2010)
35. R. Bokolia, O.P. Thakur, V.K. Rai, S.K. Sharma, K. Sreenivas, Ceram. Int. **41**, 6055–6066 (2015)
36. W.F. Liu, X.B. Ren, Phys. Rev. Lett. **103**, 257602 (2009)
37. P. Wang, Y.X. Li, Y.Q. Lu, J. Eur. Ceram. Soc. **31**, 2005–2012 (2011)
38. D.Z. Xue, Y.M. Zhou, H.X. Bao, C. Zhou, J.H. Gao, X.B. Ren, J. Appl. Phys. **109**, 054110 (2011)
39. J.P. Praveen, T. Karthik, A.R. James, E. Chandrakala, S. Asthana, D. Das, J. Eur. Ceram. Soc. **35**, 1785–1798 (2015)
40. G.B. Kumar, S. Buddhudu, Ceram. Int. **36**, 1857–1861 (2010)
41. Z.C. Ling, H.R. Xia, W.L. Liu, H. Han, X.Q. Wang, S.Q. Sun, D.G. Ran, L.L. Yu, Mater. Sci. Eng. B **128**, 156–160 (2006)
42. B.A. Golda, A. Marikan, D.P. Padiyan, Ceram. Int. **37**, 3731–3735 (2011)
43. Y. Zhang, H.J. Sun, W. Chen, Ceram. Int. **41**, 8520–8532 (2015)
44. J.G. Hao, W.F. Bai, W. Li, J.W. Zhai, J. Am. Ceram. Soc. **95**, 1998–2006 (2012)
45. H.Y. Park, J.Y. Choi, M.K. Choi, K.H. Cho, S. Nahm, H.G. Lee, H.W. Kang, J. Am. Ceram. Soc. **91**, 2374–2377 (2008)
46. H.Y. Park, C.W. Ahn, K.H. Cho, S. Nahm, H.G. Lee, H.W. Kang, D.H. Kim, K.S. Park, J. Am. Ceram. Soc. **90**, 4066–4069 (2007)
47. M. Jiang, Q. Lin, D.M. Lin, Q.J. Zheng, X.M. Fan, X.C. Wu, H.L. Sun, Y. Wan, L. Wu, J. Mater. Sci. **48**, 1035–1041 (2013)
48. C.C. Leu, C.Y. Chen, C.H. Chien, M.N. Chang, F.Y. Hsu, C.T. Hu, Appl. Phys. Lett. **82**, 3493–3495 (2003)